

# SOLUTE TRANSPORT IN SIMULATED CONDUCTIVITY FIELDS UNDER DIFFERENT IRRIGATIONS

By Dong Wang,<sup>1</sup> Scott R. Yates,<sup>2</sup> Jirka Simunek,<sup>3</sup> and Martinus T. van Genuchten<sup>4</sup>

**ABSTRACT:** The interactive effect of irrigation methods and spatial variability of saturated hydraulic conductivity ( $K_s$ ) on solute transport was determined with the combined use of a two-dimensional deterministic solute transport model and a stochastic parameter generator. In a homogeneous  $K_s$  field, the time required to infiltrate a prescribed amount of water or chemical increased from sprinkler to furrow to drip irrigation. Furrow irrigation appeared to leach the chemical more rapidly than either drip or sprinkler irrigation. Assuming the spatial distribution of  $K_s$  to be a stationary stochastic process, increased spatial variability in  $K_s$  reduced the infiltration rate. When  $K_s$  is spatially correlated, sprinkler irrigation appeared to be less susceptible to cause ground-water contamination than furrow or drip irrigation. The concentration distributions in the uncorrelated  $K_s$  field were not very different from those in the homogeneous field.

## INTRODUCTION

The presence of pesticides and fertilizers in ground water has become an increasing problem in modern irrigated agriculture. Contamination of ground water is to be expected when a substantial fraction of surface-applied chemical is leached out of soil root-zone. Transport of the chemicals in the soil is affected by many factors including soil physical, chemical, and hydrologic properties; soil surface microrelief; and irrigation practices (Wallach et al. 1991). While soil hydraulic parameters such as capillary head, moisture content, and parameters for describing the retention characteristics are fundamental to a soil and important to water and solute transport (Mantoglou and Gelhar 1987), saturated hydraulic conductivity is a parameter that directly translates the hydraulic characteristics of a soil to the transport processes. This paper examines the interactive effect of combinations of different irrigation methods with spatially variable saturated hydraulic conductivity fields on the subsurface transport of nonsorbing chemicals using both stochastic and deterministic modeling approaches. The porous medium is assumed to be either an unknown realization of a random field or a field that is subjected to some prescribed degree of spatial correlation. Parameter fields (e.g., saturated hydraulic conductivity) are described as stationary stochastic processes, and a deterministic solute transport model is used to estimate two-dimensional spatial distributions of the solute concentration.

Irrigation is one of the main factors governing the fate and transport of agrochemicals in arid and semiarid region soils (Yaron et al. 1985). Because most irrigation methods apply water at the soil surface (except subsurface drip), differences between irrigation methods are mainly a consequence of the input boundary conditions that define how water and surface-applied chemicals are transferred into the underlying semiinfinite soil profile. Due to historic, technical, and economic reasons, the most commonly applied irrigation methods in arid

and semiarid agricultural regions include sprinkler, furrow, and drip irrigation. Neglecting the effect of application nonuniformity, sprinkler irrigation is designed to apply water over the entire soil surface in a way similar to rainfall. Infiltration and solute transport under sprinkler irrigation most closely approximate one-dimensional flow. By contrast, furrow irrigation delivers water from geometrically well-defined field furrows through gravitational force (low pressure). Solute transport from the surface furrows would be generally a two-dimensional process with a ponded surface condition. In drip irrigation, water and dissolved chemicals, if any, are applied through evenly spaced point sources (emitters). Transport and redistribution of water or solutes from these surface point sources would create a three-dimensional flow regime. However, the emitters in many drip irrigated row crops are now being replaced with drip tapes having closely spaced openings (2–6 per m). Surface wetting from such drip systems leads to continuously wetted strips centered at the crop rows. Flow in this case is still two-dimensional, except that the surface boundary is not ponded as for furrow irrigation and the source of water and dissolved solute is located at the top of crop rows. How different irrigation methods would affect solute transport is not well understood. Limited publications on the effects of irrigation methods on solute transport include Troiano et al. (1993), who found more leaching of herbicide atrazine in a furrow irrigated soil than in a sprinkler irrigated soil. No literature is found on the interactive effect of irrigation methods and soil heterogeneity on solute transport.

Quantitative descriptions of chemical transport have been well advanced for soils with homogeneous medium properties (van Genuchten and Shouse 1989). Experimental and theoretical studies suggest, however, that deterministic solutions of transport models may not represent the field conditions, mostly due to field-scale variability in hydraulic parameters such as hydraulic conductivity (Sudicky 1986; Tseng and Jury 1994).

The saturated hydraulic conductivity ( $K_s$ ) has been found to be spatially variable for many natural porous media, including soil. Many studies have been carried out in efforts to understand how  $K_s$  changes in space, including methods for characterizing a variable  $K_s$  field. Wierenga et al. (1991) found that the hydraulic conductivity of a saturated field soil ranged from 1.4 to 6,731 cm/d. However, despite the wide range in conductivity values, they observed a relatively homogeneous wetting front, thus indicating the absence of preferential flow. To describe the variable nature of field saturated hydraulic conductivity over space, scaling has been adopted by many researchers (Tillotson and Nielsen 1984; Neuman 1990; Warrick 1990; Vogel et al. 1991; Dagan 1994). This technique generally evolved from the early work of Miller and Miller (1956) on microscopic geometric similitude. Other stochastic ap-

<sup>1</sup>Postdoctoral Soil Physicist and Agric. Engr., Phys. and Pesticide Res. Unit, U.S. Salinity Lab., USDA-ARS, 450 W. Big Springs Rd., Riverside, CA 92507-4617.

<sup>2</sup>Soil Physicist and Envir. Sci., Phys. and Pesticide Res. Unit, U.S. Salinity Lab., USDA-ARS, 450 W. Big Springs Rd., Riverside, CA.

<sup>3</sup>Soil Physicist and Modeler, Phys. and Pesticide Res. Unit, U.S. Salinity Lab., USDA-ARS, 450 W. Big Springs Rd., Riverside, CA.

<sup>4</sup>Res. Leader, Phys. and Pesticide Res. Unit, U.S. Salinity Lab., USDA-ARS, 450 W. Big Springs Rd., Riverside, CA.

Note. Discussion open until March 1, 1998. To extend the closing date one month, a written request must be filed with the ASCE Manager of Journals. The manuscript for this paper was submitted for review and possible publication on December 6, 1996. This paper is part of the *Journal of Irrigation and Drainage Engineering*, Vol. 123, No. 5, September/October, 1997. ©ASCE, ISSN 0733-9437/97/0005-0336-0343/\$4.00 + \$.50 per page. Paper No. 13475.

proaches in characterizing the heterogeneous nature of  $K_s$ , include Monte-Carlo (Freeze 1980), turning bands (Tompson et al. 1989), and many other methods. A log-normal probability density function has generally been assumed for  $K_s$  values (Persaud et al. 1985; Yeh et al. 1985; Rubin 1990). Rather than assuming a random distribution of log-normally transformed  $K_s$  values, spatially structured (autocorrelated) saturated hydraulic conductivity fields have been used in the simulation of water infiltration in heterogeneous soils (El-Kadi 1987; Matias et al. 1989; Tseng and Jury 1993). Using autocorrelated  $K_s$  fields, Freeze (1980) simulated the hydrology of a hillslope and concluded that the spatially structured  $K_s$  played a significant role in subsurface hydrology.

The development of simulation models has greatly enhanced our quantitative description and prediction of solute transport in the unsaturated zone. These models, with variable degrees of sophistication, include LEACHM (Wagenet and Hutson 1987), GLEAMS (Knisel et al. 1989), PRZM (Carsel et al. 1984), RZWQM ("Root" 1992), and more recently CSUID (Garcia et al. 1995). Although they remain useful tools in research and management, most of these deterministic models are designed such that they are not easily modified to include spatially and temporally varying soil hydraulic parameters. A recently developed deterministic finite-element model, CHAIN\_2D (Simunek and van Genuchten 1994), for simulating the two-dimensional movement of water, heat, and multiple solutes in variably saturated porous media is written in a way that one can easily incorporate spatially varying hydraulic parameters (including  $K_s$ ) as scaled variables. Hence, CHAIN\_2D is the transport model used in this research.

The following specific objectives are addressed in this study. First, we are interested in the transport and concentration distribution of solute when the soil is subjected to sprinkler, furrow, or drip irrigation. Next, we would like to know the behavior of solutes in soils that have either a homogeneous saturated hydraulic conductivity value or conductivities that are either spatially autocorrelated or uncorrelated. Finally, we hope that by gaining more insight about how solutes move and distribute under different irrigation and  $K_s$  fields, we can better select the appropriate irrigation method to minimize the potential for ground-water contamination.

## METHODS

### Generation of Two-Dimensional Autocorrelated and Uncorrelated $K_s$ Fields

Two major steps were involved in the methods development. First we needed to generate the two-dimensional saturated hydraulic conductivity fields. An autocorrelated conductivity field was generated by adding random frequency harmonics sampled from a spectral density function using the Monte-Carlo technique. The theory for this procedure was proposed by Mejia and Rodriguez-Iturbe (1974) and a FORTRAN code was modified from El-Kadi (1986) to perform the parameter generation. The generated conductivity fields, both the autocorrelated and uncorrelated, were log-normally distributed, and the same fields (from the same realizations of a Monte-Carlo simulation) were used in simulating sprinkler, furrow, and drip irrigation conditions. To generate the two-dimensional fields for the saturated hydraulic conductivity, we assumed that  $K_s$  can be described with a stationary log-normal probability density function. If we define a parameter  $Y$  such that

$$Y = \ln(K_s) \quad (1)$$

then  $Y$  should follow a normal distribution function. We further assumed that the parameter  $Y$  has an autocorrelation structure given by

$$\rho_Y(l) = e^{-\lambda_Y |l|} \quad (2)$$

where  $\rho_Y(l)$  = autocorrelation function as of lag  $l$ ; and  $\lambda_Y$  = an autocorrelation parameter (correlation length =  $1/\lambda_Y$ ). The values of  $Y$  are, therefore, generated from the population  $N[\mu_Y, \sigma_Y; \lambda_Y]$ , in which  $\mu_Y$  and  $\sigma_Y$  are, respectively, the mean and standard deviation of the population.

Procedures for generating autocorrelated and uncorrelated conductivity fields have been described in detail by Freeze (1980) and El-Kadi (1986). We used the original generating algorithm given by Mejia and Rodriguez-Iturbe (1974). One correction was made in the procedure, compared to Freeze (1980) and El-Kadi (1986). The residuals  $\epsilon_{ij}$  from a stochastic process  $N[0, 1; \lambda_Y]$ , where subscripts  $i = 1, 2, \dots, I; j = 1, 2, \dots, J$  denote the grid for the two-dimensional field of  $K_s$  values to be generated, were taken as

$$\epsilon_{ij} = \epsilon(x_i, z_j) = \left(\frac{2}{N}\right)^{1/2} \sum_{m=1}^N \cos[W_m(x_i \cos \gamma_m + z_j \sin \gamma_m) + \phi_m] \quad (3a)$$

rather than

$$\epsilon_{ij} = \epsilon(x_i, z_j) = \left(\frac{2}{N}\right)^{1/2} \sum_{m=1}^N \cos[W_m(x_i \sin \gamma_m + z_j \cos \gamma_m) + \phi_m] \quad (3b)$$

where  $x_i$  and  $z_j$  = horizontal and vertical directions of the two-dimensional field;  $N \geq 50$ ;  $\gamma_m$  and  $\phi_m$  are chosen from a uniform distribution over the range  $0-2\pi$  or  $U[0, 2\pi]$ ; and  $W_m$  is given by

$$W_m = \lambda_Y \left\{ \left[ \frac{1}{1 - G(W_m)} \right]^2 - 1 \right\}^{1/2} \quad (4)$$

In (4),  $G(W_m)$  is chosen from a uniform distribution over the range  $0-1$ . Eq. (3a) should be the correct form for  $\epsilon_{ij}$  because the product of  $[x_i, z_j]$  and the transpose of  $[\cos \gamma_m \sin \gamma_m]$  is  $(x_i \cos \gamma_m + z_j \sin \gamma_m)$ , which is further multiplied by  $W_m$  according to Eq. (61) from Mejia and Rodriguez-Iturbe (1974). We also performed a numerical comparison in which using (3a) generated  $\epsilon_{ij}$  conformed to  $N[0, 1; \lambda_Y]$ . However, using (3b) and the same sets of  $x_i, z_j, W_m, \gamma_m$ , and  $\phi_m$  data, the mean of generated  $\epsilon_{ij}$  was about 8.6 for  $x_i = z_j$ , 6.9 for  $x_i = 10z_j$  or  $z_j = 10x_i$ , and 0.2 for  $x_i = 100z_j$  or  $z_j = 100x_i$ , respectively. Discrepancies of (3b) from (3a) were probably only typographic errors in Freeze (1980) since the generated  $K_s$  had a mean similar to the input ( $10^{-5}$  m/s). In El-Kadi (1986), however, the generated  $K_s$  had a mean that was many times larger than the unit input.

The input parameters for generating the two-dimensional  $K_s$  fields are the mean ( $\mu_Y$ ) and standard deviation ( $\sigma_Y$ ) of the population and the autocorrelation parameter  $\lambda_Y$ . The values of  $\mu_Y$  and  $\sigma_Y$  are calculated from the following equations (Warwick and Nielsen 1980):

$$\sigma_Y = \left[ \ln \left( \frac{\sigma_{K_s}^2}{\mu_{K_s}^2} + 1 \right) \right]^{1/2} \quad (5)$$

and

$$\mu_Y = \ln \mu_{K_s} - \frac{1}{2} \sigma_Y^2 \quad (6)$$

where  $\mu_{K_s}$  and  $\sigma_{K_s}$  = mean and standard deviation, respectively, of the log-normally distributed saturated hydraulic conductivity before transformation. The points at which saturated hydraulic conductivity values are generated have the same  $x$  and  $z$  coordinates as those in the finite-element mesh used for the transport simulation.

According to a preliminary single-ring infiltrometer meas-

urement, estimated  $K$ , for an Arlington fine sandy loam (coarse-loamy, mixed, thermic Haplic Durixeralf), on which the nonsorbing tracer chemical transport and concentration distribution will be simulated, averaged about 5.0 cm/d. While Warrick and Nielsen (1980) reported that the coefficient of variation (CV) of  $K$ , ranged from 86 to 190%, we assumed a 150% CV value for this soil. Therefore, values of 5.0 and 7.5 cm/d were used for the input parameters  $\mu_K$ , and  $\sigma_K$ , respectively.

Freeze (1980) used 0.003 (1/cm) as the autocorrelation parameter  $\lambda_y$ , for ground-water flow simulations. El-Kadi and Brutsaert (1985) used, in four out of six experiments, 25% of the total length as the correlation length ( $= 1/\lambda_y$ ). Tseng and Jury (1993) applied 25–40% as the horizontal and 5–15% as the vertical correlation length. In this research, we used 25% of the horizontal length ( $= 90$  cm) as the correlation scale for both horizontal and vertical directions, which resulted in an  $\lambda_y$  value of 0.044 (1/cm).

### Solute Transport Simulated with CHAIN\_2D, Code Modification, Input Parameters, and Boundary and Initial Conditions

The next step in the method development was to simulate the flow and transport using the computer model CHAIN\_2D (Simunek and van Genuchten 1994), which numerically solves Richards' equation for water flow and the Fickian-based convection-dispersion equation for solute transport using Galerkin-type linear finite-element schemes. Simulations were carried out in a two-dimensional vertical plane (see Fig. 1 for geometry). Simulated scenarios included combinations of the three irrigation methods and three saturated hydraulic conductivity fields (including a homogeneous field). Besides solving the nonsorbing chemical concentration distribution for only one realization of the autocorrelated and uncorrelated  $K$ , field, we also obtained averaged solute concentration distributions of 50 simulations for both the autocorrelated and uncorrelated conductivity fields. This was readily achieved by modifying the CHAIN\_2D computer code to include an additional subroutine for generating the autocorrelated or uncorrelated parameters. The transport model, CHAIN\_2D, numerically

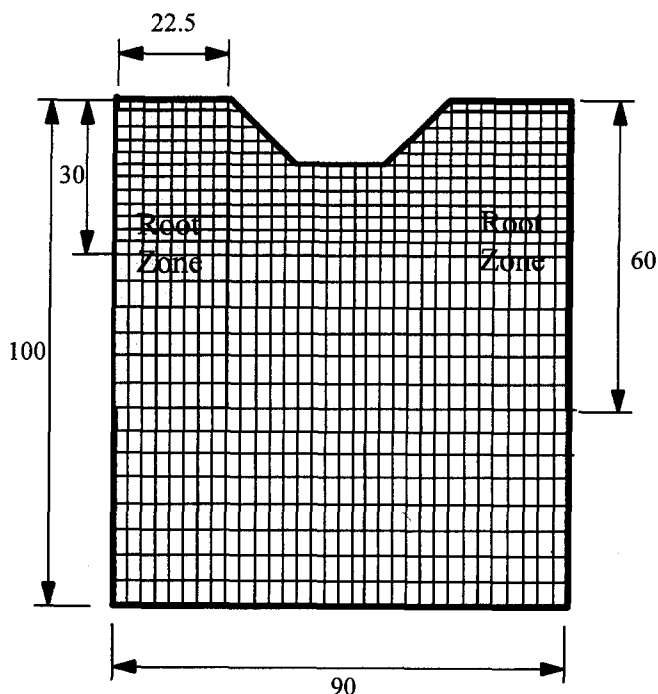


FIG. 1. Schematic of Cross-Section Subjected to Sprinkler, Furrow, and Drip Irrigation (Units in cm)

solves the partial differential equations for two-dimensional nonlinear nonequilibrium solute transport involving a first-order solute decay chain reaction during transient water flow in a variably saturated porous medium. For a nonsorbing chemical without decay and volatilization, the governing transport equation can be simplified to

$$\frac{\partial \theta C}{\partial t} = \frac{\partial}{\partial x_i} \left( \theta \mathbf{D}_{ij}^* \frac{\partial C}{\partial x_j} \right) - \frac{\partial q_i C}{\partial x_i} \quad (7)$$

where  $\theta$  = volumetric water content;  $C$  = solute concentration in soil solution;  $t$  = time;  $x_i$  and  $x_j$  = spatial coordinates;  $q_i$  represents the Darcian fluid flux density; and  $\mathbf{D}_{ij}^*$  is the dispersion coefficient tensor for the liquid phase and described as follows (Bear 1972)

$$\theta \mathbf{D}_{ij}^* = D_T |q| \delta_{ij} + (D_L - D_T) \frac{q_i q_j}{|q|} + \theta D_w \tau_w \delta_{ij} \quad (8)$$

where  $D_L$  and  $D_T$  = longitudinal and transverse dispersivity;  $\delta_{ij}$  = Kronecker delta function;  $D_w$  = molecular diffusion coefficient in free water; and  $\tau_w$  = a tortuosity factor. Dispersivity values for field conditions can range from 5 to 20 cm (Jury et al. 1991; Beven et al. 1993). In this simulation study we used 10 and 5 cm for the longitudinal and transverse dispersivity, respectively.

Variably saturated water flow was simulated using the Richards' equation with the unsaturated soil hydraulic functions described by a set of closed-form equations resembling those of van Genuchten (1980). Five parameters,  $\theta_r$ ,  $\theta_s$ ,  $\alpha$ ,  $n$ , and  $K_s$ , are used in the model. Of these,  $\theta_r$  and  $\theta_s$  represent residual and saturated volumetric soil water content;  $\alpha$  and  $n$  are characteristic hydraulic parameters of the soil. Because a mean  $K$ , value was found to be about 5.0 cm/d, the remaining four parameters were taken to be those of the silt loam G.E. 3 of van Genuchten (1980), leading to the following values:  $\theta_r = 0.131$ ,  $\theta_s = 0.396$ ,  $\alpha = 0.00423$  (1/cm), and  $n = 2.06$ .

To simulate water and solute transport under field irrigated conditions, the CHAIN\_2D model was modified by creating a new boundary code that will switch boundary conditions back and forth between an evaporative and a ponded or a flux input condition at: (1) prescribed time intervals; or (2) elapsed times when the total water or solute inflow had reached a prescribed amount. The program was also made to apply to chemigation. Chemigation has become a common practice in modern irrigation technology because of its ability to more easily control chemical input in irrigated soils. The time and duration for chemical injection was determined in a similar fashion as for water input, i.e., by starting at a prescribed time and terminating when a prescribed amount was reached. To obtain a spatially weighted concentration distribution, we averaged solute concentration for each nodal point from 50 simulation runs for both the autocorrelated and uncorrelated conductivity fields.

The boundary conditions used in the simulation are determined by the type of irrigation methods involved. For sprinkler irrigation, a flux input (36 cm/d) was used over the entire soil surface (90 cm wide). A maximum ponding depth ( $= 1.0$  cm) was permitted in the simulation. For furrow irrigation, we applied a ponded condition with a fixed depth ( $= 7.5$  cm) to areas in the bottom of the furrow (20 cm wide, including the sides of the furrow). The remainder of the surface was subjected to evaporation. For drip irrigation, water and chemical were applied to the top of the rows, assuming a wetting width of 25 cm. Because of symmetry, each side of the furrow had 12.5 cm wetting. The wetted area was assumed to be at water saturation ( $h \geq 0$ ). The remaining part of the soil surface was again subjected to evaporation.

The following fixed boundary and initial conditions were applied to all three irrigation methods. A region 45 cm wide

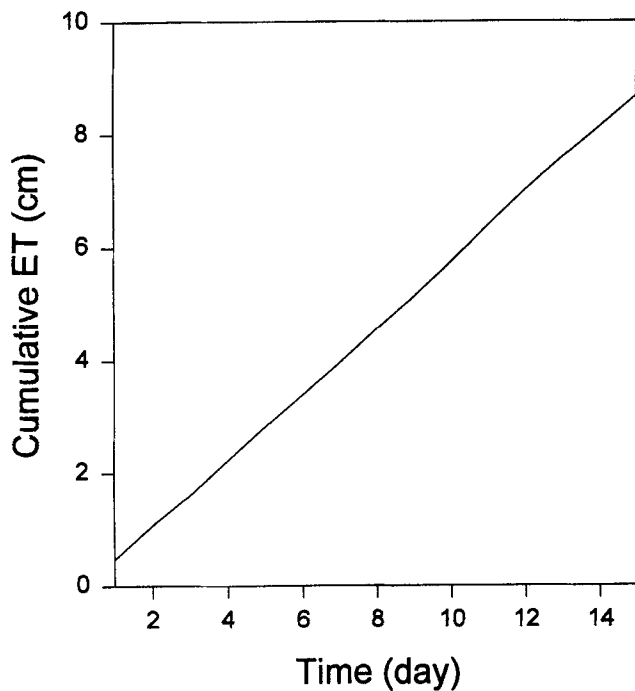


FIG. 2. Cumulative Potential Evapotranspiration (ET) Obtained from Weather Station Located on University of California-Riverside Campus; Data is from July 1–15, 1994

by 60 cm deep (excluding the surface 2.5-cm layer) beneath the top of each row was assumed to be subjected to root water uptake with a maximum transpiration rate of 0.508 cm/d (Fig. 1). This rate approximates the peak growth for dry beans in southern California. Evapotranspiration (ET) was the sum of root water uptake and surface water evaporation. We used a set of actual measured potential ET data from a California irrigation management information system's weather station located at Riverside for the input in our simulations (Fig. 2). Total irrigation and chemical injection (at unit concentration) were 6 and 3 cm for each of the three irrigation methods, respectively. Because of symmetry, a zero flux boundary condition was used for the sides of the simulation domains. A unit flux boundary condition was used for the bottom boundary. An initial soil water pressure head of  $-150$  cm was used. The simulation involved only one irrigation event, which was initiated on the fifth day, whereas the simulation itself was run for 15 d to allow sufficient time for redistribution.

## RESULTS AND ANALYSIS

Two-dimensional saturated hydraulic conductivity fields, both autocorrelated and uncorrelated, were generated using a single realization of the Monte-Carlo simulation (Fig. 3). The correlation length used in the autocorrelated case was 22.5 cm, which created bands of high conductivity regions with a band width ranging from 20 to 40 cm [Fig. 3(a)]. The realization in Fig. 3(a) exhibited lower  $K_s$  values in the upper left region of the cross section as compared to the rest of the vertical plane. In the uncorrelated case, occurrences of high and low conductivities appear to be spatially random with no trend of high or low regions [Fig. 3(b)]. Besides later multirealization averaging, these two conductivity fields were used repetitively in comparing different irrigation methods. While the results of solute transport under different irrigation methods was very dependent on the chosen realization of  $K_s$  fields, we believe the use of a randomly chosen realization was appropriate because it provided the comparison of the effect of irrigation methods on solute transport.

For homogeneous  $K_s$  field, the time needed to apply 6 cm

of water increased from sprinkler irrigation to furrow to drip irrigation (Table 1 and Fig. 4, homogeneous case). The high overall infiltration rate with the sprinkler method as compared to furrow or drip irrigation was due primarily to the available infiltration area, where the whole soil surface was subjected to infiltration for sprinkler method. In furrow irrigation, a positive head (or ponding) would increase the local infiltration flux, while the rest surface area would not contribute to infiltration. Drip irrigation had the lowest infiltration rate because of the reduced application rate and small infiltration area relative to sprinkler or furrow irrigation. Furthermore, infiltration in drip irrigation was mainly induced by capillary-driven flow. When compared on a single-realization basis, e.g., using the conductivity fields in Fig. 3, the autocorrelated field reduced the overall water inflow rate relative to that in the homogeneous conductivity field (Fig. 4). This effect is more evident for furrow irrigation, whether about twice the time is needed to infiltrate 6 cm of water in the autocorrelated hydraulic conductivity field than in the homogeneous field (Table 1). Had the high  $K_s$  regions coincided with the ponding portion of the soil surface, however, the infiltration rate would have been higher and possibly exceeded that of sprinkler irrigation. The spatially uncorrelated conductivity field also reduced the infiltration rate, but not as much as in the correlated case. This indicates that isolated high  $K_s$  values are not effective in increasing the overall infiltration rate, especially for sprinkler

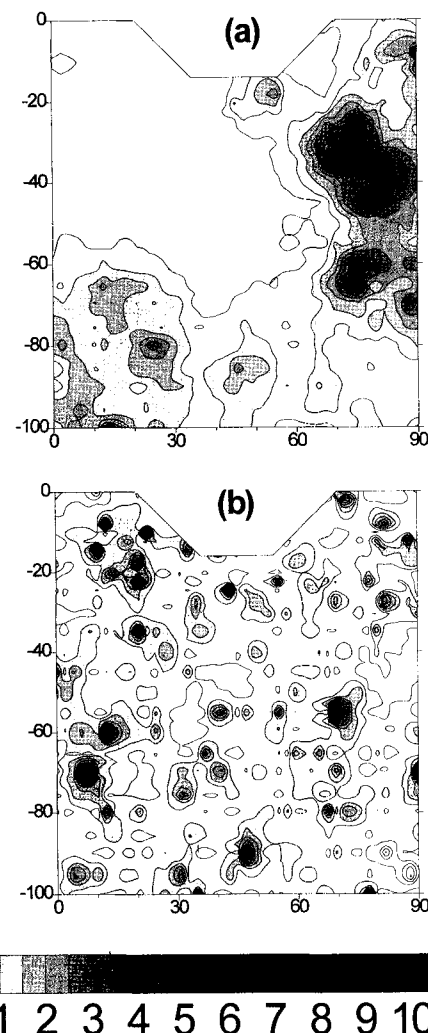
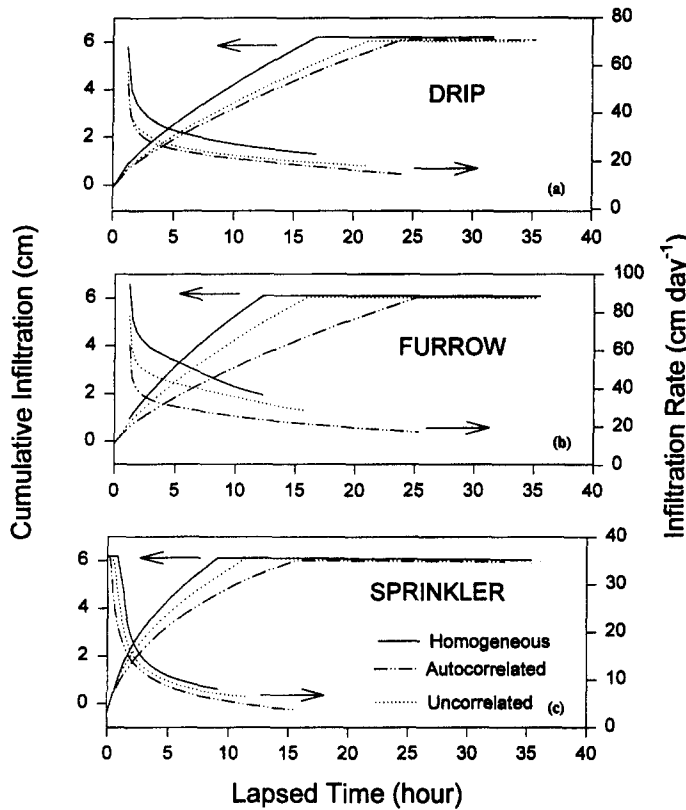


FIG. 3. Generated Saturated Hydraulic Conductivity Fields (Scaled to Mean of 5 cm/d, i.e., value of 1 corresponds to 5 cm/d) by Assuming: (a) Autocorrelated  $K_s$  with  $\lambda_v = 0.044$  (1/cm),  $\sigma_{K_s} = 5.07$  cm/d; (b) Uncorrelated  $K_s$  with  $\lambda_v \rightarrow \infty$ ,  $\sigma_{K_s} = 5.58$  cm/d (Axes in cm)

**TABLE 1. Time Taken to Infiltrate 6 cm Water and 3 cm Tracer under Combinations of Drip, Furrow, and Sprinkler Irrigation with Autocorrelated, Uncorrelated, Homogeneous Saturated Hydraulic Conductivity Fields**

Time (h) (1)	Drip			Furrow			Sprinkler		
	Autocorrelated (2)	Homogeneous (3)	Uncorrelated (4)	Autocorrelated (5)	Homogeneous (6)	Uncorrelated (7)	Autocorrelated (8)	Homogeneous (9)	Uncorrelated (10)
$t_w^*$	24.04	16.89	21.17	25.33	12.30	15.94	15.61	9.13	11.50
$t_c^*$	9.36	6.48	8.40	9.60	5.04	6.48	4.56	2.88	3.60

*t<sub>w</sub>* = Time needed to infiltrate 6 cm water; *t<sub>c</sub>* = time needed to infiltrate 3 cm tracer.



**FIG. 4. Instantaneous Accumulative Infiltration Rate for Drip, Furrow, and Sprinkler Irrigation Compared on Single-Realization Basis between Autocorrelated, Uncorrelated, and Homogeneous  $K_s$  Fields**

irrigation. A similar conclusion was made by El-Kadi (1987), who reported a reduced infiltration rate for structured hydraulic conductivity fields as compared to homogeneous media. This result is caused by the stationary process of generating two-dimensional  $K_s$  values.

Using the homogeneous  $K_s$  field as an example, vertical distribution of solute concentration profiles were obtained for each irrigation method at 2 and 10 d after the initiation of irrigation (Fig. 5). This was achieved by averaging solute concentrations within each horizontal depth increment (every 2 cm). Nonsorbing tracers traveled deeper into the soil in furrow irrigation than in drip or sprinkler irrigation, due primarily to surface ponding. These horizontally averaged concentration profiles also reflected the effects of evaporation and root water uptake on solute transport, which led to upward water and solute movement and increased solute concentrations in the soil after water had been either evaporated from the surface or uptaken by plant roots. The surface solute concentration increased from about 0.25 on the second day to 0.50 on the fourth day.

Figs. 6–8 show two-dimensional tracer concentration distributions for homogeneous, autocorrelated, and uncorrelated hydraulic conductivity fields on a single-realization basis for drip, furrow, and sprinkler irrigation, respectively. Surface-ap-

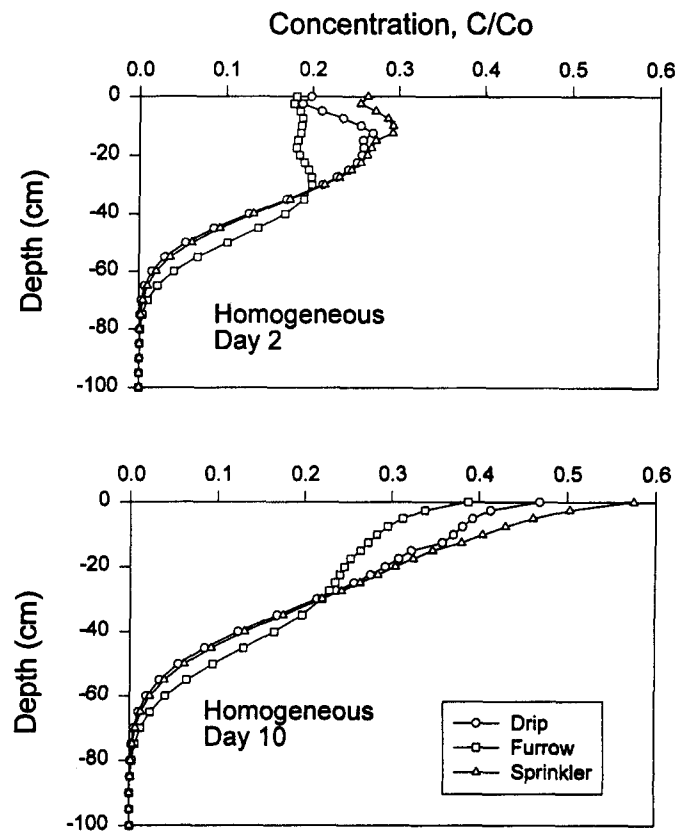


**FIG. 5. Horizontally Averaged Solute Concentrations Obtained for Homogeneous  $K_s$  Field under Drip, Furrow, and Sprinkler Irrigation, 2 (top) and 10 (bottom) d after Irrigation Started**

plied solutes always traveled farther into the profile along the high conductivity regions of the autocorrelated field. Therefore, preferential flow may occur under any of the three irrigation methods if there is a region with elevated hydraulic conductivity values. Two days after irrigation started, the center of solute mass reached a depth of about 40 cm for the drip and furrow irrigation methods, but remained at about a 20-cm depth for the sprinkler irrigation in the high conductivity regions of the autocorrelated fields (Figs. 6–8). Ten days after the initiation of irrigation, the center of solute mass was at a depth of about 30 cm for the drip and furrow irrigation methods, but moved to about a 10-cm depth for the sprinkler irrigation in the high conductivity regions of the autocorrelated fields (Figs. 6–8). Conversely, if the source for water and solute happened to occur at places where the  $K_s$  was the lowest, opposite results would have been obtained between sprinkler and other localized application methods such as furrow and drip. The relation between irrigation methods and  $K_s$  distribution indicates that water infiltration and solute transport in sprinkler irrigation is less likely affected by the spatially variable nature of saturated hydraulic conductivity than in furrow or drip irrigation. A potential practical application is the selection of irrigation methods for soils of known spatial variability. For soils with highly variable  $K_s$  values (with correlation

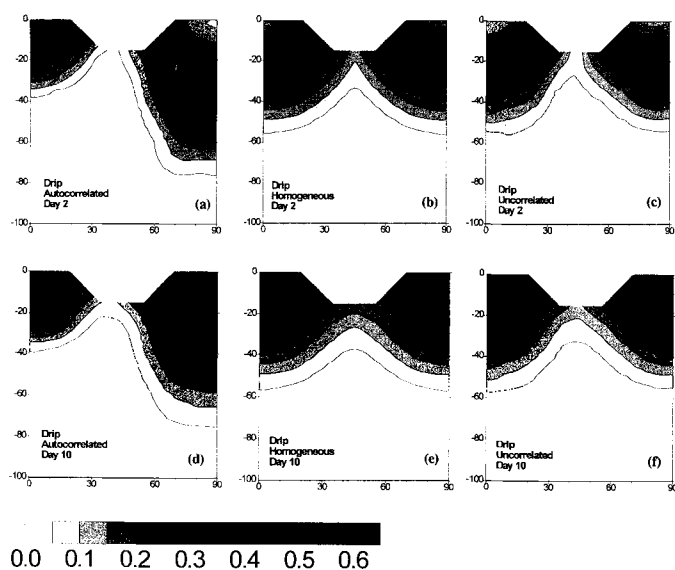


**FIG. 6. Simulated Relative Concentration Distributions at 2 and 10 d after Drip Irrigation for Homogeneous and Autocorrelated and Uncorrelated  $K_s$  Field Shown in Fig. 3**

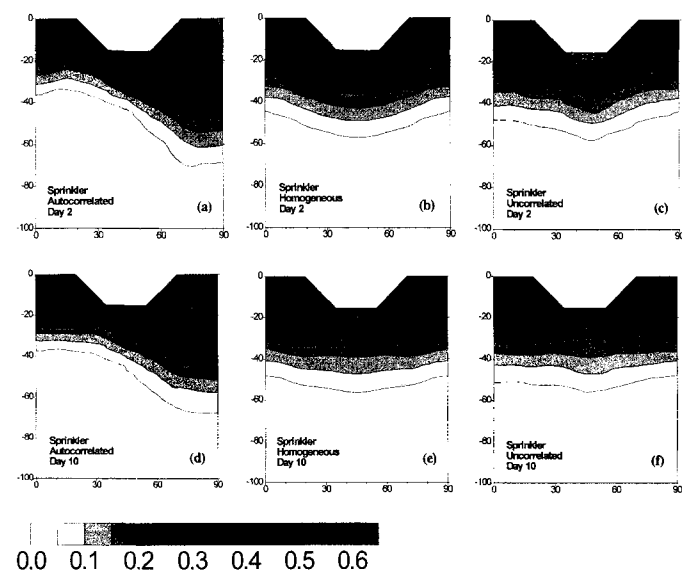


**FIG. 7. Simulated Relative Concentration Distributions at 2 and 10 d after Furrow Irrigation for Homogeneous and Autocorrelated and Uncorrelated  $K_s$  Field Shown in Fig. 3**

length in the order of furrow or emitter spacing), sprinkler irrigation should be used to reduce deep leaching and prevent ground-water contamination. The concentration distributions in the uncorrelated hydraulic conductivity field were not very different from those in the homogeneous field for all three irrigation methods. This would indicate, from a practical stand point, that different irrigation methods would unlikely create preferential movement if the  $K_s$  values of a soil is randomly distributed or correlated, but in a distance that is much smaller than the spacing between individual water and solute sources. The other factor affecting the occurrence of preferential flow is the relative difference between correlation length for  $K_s$  and local dispersion lengths for water and solute. If the correlation length is the same or smaller than the dispersion length, diffusion would dominate and advective preferential flow would unlikely to occur. The longitudinal and transverse dispersion lengths used in this study were 10 and 5 cm, respectively. The presence of surface evaporation and root water uptake tends to enhance lateral redistribution of a tracer and, hence, may limit excessive leaching. This effect can be seen by comparing

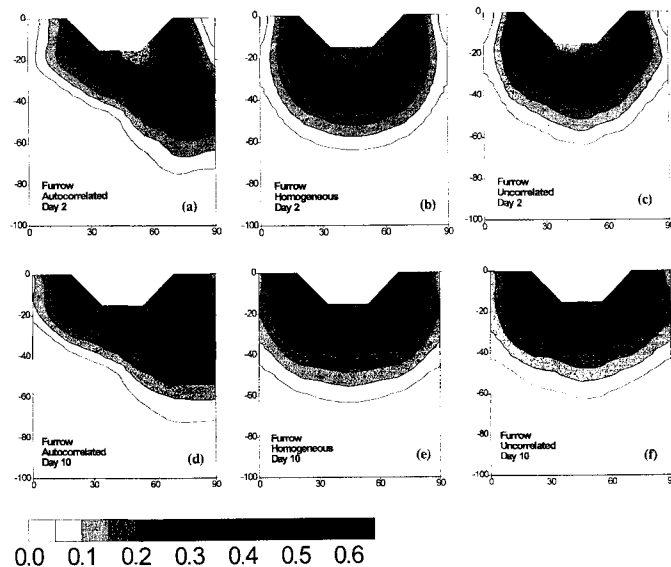


**FIG. 8. Simulated Relative Concentration Distributions at 2 and 10 d after Sprinkler Irrigation for Homogeneous and Autocorrelated and Uncorrelated  $K_s$  Field Shown in Fig. 3**

chemical distributions between 2 and 10 d after irrigation when upward and possibly lateral movement occurred and the solute was concentrated near the soil surface.

Running the transport model 50 times, each time with a different hydraulic conductivity field, we obtained 50 different solute concentration distributions. By averaging the 50 concentration values for each nodal point, we obtained a set of concentration distributions representing the mean of a stationary (or close to it) stochastic process. This multirealization averaging was performed for all three irrigation methods and for both the autocorrelated and uncorrelated scenarios. The averaged concentration distributions for both the autocorrelated and uncorrelated hydraulic conductivity field are very similar to the homogeneous field for all three irrigation methods. This is not surprising since we used the same value (5 cm/d) as the input mean  $K_s$ . Furthermore, as indicated by Freeze (1980), among the mean, standard deviation, and spatial structure, spatial structure is the least important factor determining the translocation of a solute center mass over spaces much larger than the structural correlation length. To further verify our procedure for generating log-normally distributed  $K_s$  field in conjunction with the solute transport simulation, we created a solute concentration profile similar to Fig. 13.6 from Warrick and Nielsen (1980), using the approaches described in this paper, and adopting initial and boundary conditions similar to those of Warrick and Nielsen (1980) [the pore water velocity and diffusion coefficient were the same as that used in Warrick and Nielsen (1980)]. This profile was obtained by first generating 50 log-normally distributed  $K_s$  values with a mean of 35 cm/d and standard deviation of 58.2 cm/d. Then, similar to our homogeneous case, we ran the transport model 50 times, each time with a fixed  $K_s$  value sequentially chosen from the 50. After taking every nodal point for an average of the 50 solute concentrations and plotting the average values versus depth, we obtained Fig. 9(a). The deterministic curve was for the mean  $K_s$  (35 cm/d). Comparing Fig. 9(a) with Fig. 13.6 from Warrick and Nielsen (1980), we noticed the same trend in that the mean value curve showed a lower concentration than the deterministic curve at shallow depths, with the reverse results occurring at deeper depths. This effect of averaging solute concentrations was not present in our two-dimensional simulation [Fig. 9(b)], probably second of two reasons. First, solute transport for each realization was based on a two-dimensional  $K_s$  field for our case and on a single value

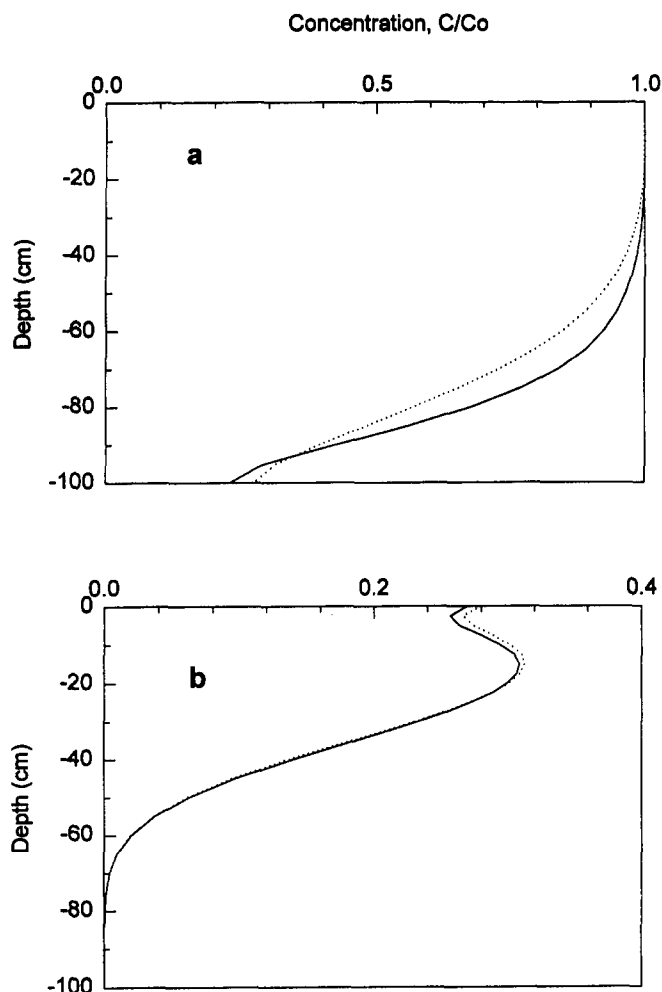


**FIG. 9. Mean Solute Concentration versus Depth: (a) 5 d after Starting Continuous Solute Input; (b) 2 d after Completing 3-cm Pulse Input; Solid Line Represents Deterministic Solutions (with Mean  $K_s$ ); Dotted Line Is Average of 50 Realizations with Means of 35 and 5 and Standard Deviations of 58 and 7.5 cm/d for (a) and (b), Respectively**

for Warrick and Nielsen (1980). Next, Warrick and Nielsen (1980) used a continuous solute source without upward (evaporation) or lateral driving forces (root water uptake) for solute and water movement. While results and conclusions by Warrick and Nielsen (1980) are theoretically correct, we believe that in field conditions small-scaled variability in soil hydrologic properties may not play a very significant role in terms of transporting the center mass of a surface-applied solute pulse.

Although the mean remained about the same, the cv of the solute concentration from the 50 realizations showed a consistent increase with depth for both the autocorrelated and uncorrelated conditions (Fig. 10). Because different ranges in  $K_s$  would occur in regions bounded by the correlation length, autocorrelated  $K_s$  fields tended to have higher variations than the uncorrelated fields. The magnitude of variation increased from sprinkler to drip to furrow irrigation. This result further indicated the presence of preferential flow at deeper depths in furrow (or drip) than in sprinkler irrigation.

## SUMMARY AND CONCLUSIONS

Assuming a fixed amount of water and chemical input, hydraulic parameters and solute concentration distributions under drip, furrow, and sprinkler irrigation were obtained with a deterministic solute transport model. Because of differences in infiltration area and surface ponding depth, sprinkler irrigation

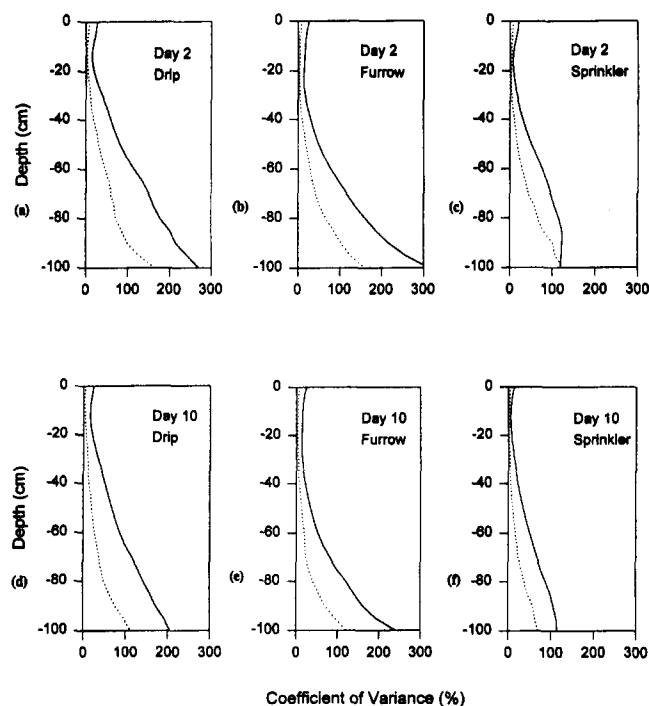


**FIG. 10. Coefficient of Variance of Solute Concentrations (at  $x = 67.5$  cm) for 50 Realizations of Autocorrelated (Solid Lines) and Uncorrelated (Dotted Lines)  $K_s$  Fields under Drip, Furrow, and Sprinkler Irrigation**

required the least amount of time to infiltrate the prescribed amount of water or chemical, followed by furrow and drip irrigation. As compared to sprinkler irrigation, drip irrigation took 85% more time to infiltrate the same prescribed amount of water and solute. Furrow irrigation appeared to leach the tracer chemicals more efficiently than either drip or sprinkler irrigation methods. Two days after starting irrigation, solute concentrations in the furrow irrigated soil were 40% lower than those in either the drip- or sprinkler-irrigated soils at 15 cm depth and 90% higher at 50 cm depth.

Spatial variability in  $K_s$  was simulated using Monte-Carlo techniques by generating two-dimensional fields of variable conductivity values. Simulated scenarios included autocorrelated and uncorrelated log-normally distributed hydraulic conductivity fields. Solute transport and concentration distributions under spatially variable conductivity fields were estimated with the solute transport model. Results indicate that for a stationary stochastic process, spatial variability in hydraulic conductivity reduces infiltration rate. Surface applied tracers traveled deeper into the soil through the high conductivity regions of the autocorrelated field under all three irrigation methods. The concentration distributions for the uncorrelated hydraulic conductivity field were not very different from those for the homogeneous  $K_s$  field. When averaging solute concentrations over multiple realizations of the simulation, distributions for the autocorrelated and uncorrelated hydraulic conductivity fields were found to be very similar to those for the homogeneous  $K_s$  field. This may indicate that spatially variable hydraulic conductivities may not have a significant effect on transferring the center mass of a surface applied nonsorbing chemical over a large area, compared to other factors such as preferential flow through macropores. Nevertheless, when subject to spatial variation, solute concentrations vary as depth increases. The variation in solute concentration was higher in the autocorrelated than in the uncorrelated  $K_s$  fields. It also indicates that sprinkler irrigation has the least potential for preferential transport of water and solutes in soils with structured hydraulic conductivity fields.

## APPENDIX I. REFERENCES

- Bear, J. (1972). *Dynamics of fluid in porous media*. Elsevier Science Publishing Co., Inc., New York, N.Y.
- Beven, K. J., Henderson, D. E., and Reeves, A. D. (1993). "Dispersion parameters for undisturbed partially saturated soil." *J. Hydro.*, Amsterdam, The Netherlands, 143(3), 19–43.
- Carsel, R. F., Smith, C. N., Mulkey, L. A., Dean, J. D., and Jowise, P. (1984). *User's manual for the pesticide root zone model (PRZM): Release 1, Rep. EPA-600/3-84-109*, U.S. EPA, Envir. Res. Lab., Athens, Ga.
- Dagan, G. (1994). "The significance of heterogeneity of evolving scales to transport in porous formations." *Water Resour. Res.*, 30(12), 3327–3336.
- El-Kadi, A. I. (1986). "A computer program for generating two-dimensional fields of autocorrelated parameters." *Ground Water*, 24(5), 663–667.
- El-Kadi, A. I. (1987). "Variability of infiltration under uncertainty in unsaturated zone parameters." *J. Hydro.*, Amsterdam, The Netherlands, 90(5), 61–80.
- El-Kadi, A. I., and Brutsaert, W. (1985). "Applicability of effective parameters for unsteady flow in nonuniform aquifers." *Water Resour. Res.*, 21(2), 183–198.
- Freeze, R. A. (1980). "A stochastic-conceptual analysis of rainfall-runoff processes on a hillslope." *Water Resour. Res.*, 16(2), 391–408.
- Garcia, L. A., Manguerra, H. B., and Gates, T. K. (1995). "Irrigation-drainage design and management model: Development." *J. Irrig. and Drain. Engrg.*, ASCE, 121(1), 71–82.
- Jury, W. A., Gardner, W. R., and Gardner, W. H. (1991). *Soil Physics*. John Wiley & Sons, Inc., New York, N.Y.
- Knisel, W. G., Leonard, R. A., and Davis, F. M. (1989). *GLEAMS User Manual*. Southeast Watershed Research Lab., Tifton, Ga.
- Mantoglou, A., and Gelhar, L. W. (1987). "Capillary tension head variance, mean soil moisture content, and effective specific soil moisture capacity of transient unsaturated flow in stratified soils." *Water Resour. Res.*, 23(1), 47–56.
- Matias, P., Correia, F. N., and Pereira, L. S. (1989). "Influence of spatial variability of saturated hydraulic conductivity on the infiltration process." *Unsaturated flow in hydrologic modeling: Theory and practice*, H. J. Morel-Seytoux, ed., Kluwer Academic Publishers, London, U.K., 455–67.
- Mejia, J. M., and Rodriguez-Iturbe, I. (1974). "On the synthesis of random field sampling from the spectrum: An application to the generation of hydrologic spatial processes." *Water Resour. Res.*, 10(4), 705–711.
- Miller, E. E., and Miller, R. D. (1956). "Physical theory of capillary flow phenomena." *J. Appl. Phys.*, 27(4), 324–332.
- Neuman, S. P. (1990). "Universal scaling of hydraulic conductivities and dispersivities in geologic media." *Water Resour. Res.*, 26(8), 1749–1758.
- Persaud, N., Giraldez, J. V., and Chang, A. C. (1985). "Monte-Carlo simulation of non-interacting solute transport in a spatially heterogeneous soil." *Soil Sci. Soc. Am. J.*, 49(3), 562–568.
- "Root Zone Water Quality Model, version 1.0." (1992). *GPSR Tech. Rep. No. 3*, Agric. Res. Svc., Great Plains Systems Research Unit, Ft. Collins, Colo.
- Rubin, Y. (1990). "Stochastic modeling of macrodispersion in heterogeneous porous media." *Water Resour. Res.*, 26(1), 133–142.
- Simunek, J., and van Genuchten, M. T. (1994). "The CHAIN-2D code for simulating the two-dimensional movement of water, heat, and multiple solutes in variably-saturated porous media, Version 1.1." *Res. Rep. No. 136*. U.S. Salinity Laboratory, USDA-ARS, Riverside, Calif.
- Sudicky, E. A. (1986). "A natural-gradient experiment on solute transport in a sand aquifer: Spatial variability of hydraulic conductivity and its role in the dispersion process." *Water Resour. Res.*, 22(13), 2069–2082.
- Tillotson, P. M., and Nielsen, D. R. (1984). "Scale factors in soil science." *Soil Sci. Am. J.*, 48(5), 953–959.
- Tompson, A. F. B., Ababou, R., and Gelhar, L. W. (1989). "Implementation of the three-dimensional turning bands random field generator." *Water Resour. Res.*, 25(10), 2227.
- Troiano, J., Garretson, C., Krauter, C., Brownell, J., and Huston, J. (1993). "Influence of amount and method of irrigation water application on leaching of atrazine." *J. Envir. Qual.*, 22(2), 290–298.
- Tseng, P. H., and Jury, W. A. (1993). "Simulation of field measurement of hydraulic conductivity in unsaturated heterogeneous soil." *Water Resour. Res.*, 29(7), 2087–2099.
- Tseng, P. H., and Jury, W. A. (1994). "Comparison of transfer function and deterministic modeling of area-averaged solute transport in a heterogeneous field." *Water Resour. Res.*, 30(7), 2051–2063.
- van Genuchten, M. T. (1980). "A closed-form equation for predicting the hydraulic conductivity of unsaturated soils." *Soil Sci. Soc. Am. J.*, 44(5), 892–898.
- van Genuchten, M. T., and Shouse, P. J. (1989). "Solute transport in heterogeneous field soils." *Intermedia pollutant transport: Modeling and field measurement*, D. T. Allen, Y. Cohen, and I. R. Kaplan, eds., Plenum Publishing Corp., New York, N.Y., 177–187.
- Vogel, T., Cislerova, M., and Hopmans, J. W. (1991). "Porous media with linearly variable hydraulic properties." *Water Resour. Res.*, 27(10), 2735–2741.
- Wagenet, R. J., and Hutson, J. L. (1987). *LEACHM: A finite-difference model for simulating water, salt, and pesticide movement in the plant root zone, continuum 2*. New York State Resources Institute, Cornell Univ., Ithaca, N.Y.
- Wallach, R., Israeli, M., and Zaslavsky, D. (1991). "Small perturbation solution for steady nonuniform infiltration into soil surface of a general shape." *Water Resour. Res.*, 27(7), 1665–1670.
- Warrick, A. W. (1990). "Application of scaling to the characterization of spatial variability in soils." *Scaling in Soil Physics: Principles and Applications*, D. Hillel and D. E. Elrick, eds., SSSA Special Publ. No. 25, Soil Sci. Soc. Am., Madison, Wis., 39–51.
- Warrick, A. W., and Nielsen, D. R. (1980). "Spatial variability of soil physical properties in the field." *Applications of Soil Physics*, D. Hillel, ed., Academic Press, Inc., New York, N.Y., 319–44.
- Wierenga, P. J., Hills, R. G., and Hudson, D. B. (1991). "The Las Cruces Trench site: Characterization, experimental results, and one-dimensional flow predictions." *Water Resour. Res.*, 27(10), 2695–2705.
- Yaron, B., Gerstl, Z., and Spencer, W. F. (1985). "Behavior of herbicides in irrigated soils." *Adv. Soil Sci.*, 3, 121–211.
- Yeh, T. C. J., Gelhar, L. W., and Gutjahr, A. L. (1985). "Stochastic analysis of unsaturated flow in heterogeneous soils. 1: Statistically isotropic media." *Water Resour. Res.*, 21(4), 447–456.

## APPENDIX II. NOTATION

The following symbols are used in this paper:

- $C$  = solute concentration;  
 $CV$  = coefficient of variance;  
 $D_L, D_T$  = longitudinal and transverse dispersivity;  
 $D_w$  = molecular diffusion coefficient in free water;  
 $\mathbf{D}_{ij}^*$  = dispersion coefficient tensor;  
 $G(W_m)$  = values chosen from uniform distribution over the range 0–1;  
 $K_s$  = saturated hydraulic conductivity;  
 $q, q_i, q_j$  = components of Darcian fluid flux density;  
 $t$  = time;  
 $W_m$  = dummy variable;  
 $x_i$  = coordinate in horizontal direction of two-dimensional field;  
 $x_j, z_i$  = coordinate in vertical direction of two-dimensional field;  
 $Y$  = parameter that was used to transform  $K_r$  from log-normal to normal distribution;  
 $\alpha, n$  = characteristic hydraulic parameters of soil;  
 $\gamma_m, \phi_m$  = random angular variables chosen from uniform distribution over the range 0– $2\pi$  or ( $U[0, 2\pi]$ );  
 $\delta_{ij}$  = Kronecker delta function;  
 $\epsilon_{ij}$  = residuals from a stochastic process of  $N[0, 1; \lambda_y]$ ;  
 $\theta$  = volumetric soil water content;  
 $\theta_r, \theta_s$  = residual and saturated volumetric soil water content;  
 $\lambda_y$  = autocorrelation parameter;  
 $\mu_K, \sigma_K$  = mean and standard deviation of log-normally distributed saturated hydraulic conductivity;  
 $\mu_Y, \sigma_Y$  = mean and standard deviation of population for  $Y$ ;  
 $\rho_Y(l)$  = autocorrelation function as of lag  $l$ ; and  
 $\tau_w$  = tortuosity factor in water and solute transport.